



## Molecular Crystals and Liquid Crystals Science and Technology. Section A. Molecular Crystals and Liquid Crystals

Publication details, including instructions for authors and subscription information:

<http://www.tandfonline.com/loi/gmcl19>

### Optically Induced EPR in Halogen-Bridged Linear Chain Complex [Pt(En)<sub>2</sub>][Pt(en)<sub>2</sub>Cl<sub>2</sub>](ClO<sub>4</sub>)<sub>4</sub>, en=NH<sub>2</sub>CH<sub>2</sub>CH<sub>2</sub>NH<sub>2</sub>

Noritaka Kuroda<sup>a</sup>, Masamichi Sakai<sup>a</sup>, Masashi Suezawa<sup>a</sup>,  
Yuichiro Nishina<sup>a</sup>, Koji Sumino<sup>a</sup> & Masahiro Yamashita<sup>a,b</sup>

<sup>a</sup> Institute for Materials Research, Tohoku University, Sendai, 980, Japan

<sup>b</sup> College of General Education, Nagoya University, Nagoya, 464-01, Japan

Version of record first published: 24 Sep 2006.

To cite this article: Noritaka Kuroda , Masamichi Sakai , Masashi Suezawa , Yuichiro Nishina , Koji Sumino & Masahiro Yamashita (1992): Optically Induced EPR in Halogen-Bridged Linear Chain Complex [Pt(En)<sub>2</sub>][Pt(en)<sub>2</sub>Cl<sub>2</sub>](ClO<sub>4</sub>)<sub>4</sub>, en=NH<sub>2</sub>CH<sub>2</sub>CH<sub>2</sub>NH<sub>2</sub> , Molecular Crystals and Liquid Crystals Science and Technology. Section A. Molecular Crystals and Liquid Crystals, 216:1, 169-174

To link to this article: <http://dx.doi.org/10.1080/10587259208028768>

PLEASE SCROLL DOWN FOR ARTICLE

Full terms and conditions of use: <http://www.tandfonline.com/page/terms-and-conditions>

This article may be used for research, teaching, and private study purposes. Any substantial or systematic reproduction, redistribution, reselling, loan, sub-licensing, systematic supply, or distribution in any form to anyone is expressly forbidden.

The publisher does not give any warranty express or implied or make any representation that the contents will be complete or accurate or up to date. The

accuracy of any instructions, formulae, and drug doses should be independently verified with primary sources. The publisher shall not be liable for any loss, actions, claims, proceedings, demand, or costs or damages whatsoever or howsoever caused arising directly or indirectly in connection with or arising out of the use of this material.

OPTICALLY INDUCED EPR IN HALOGEN-BRIDGED LINEAR CHAIN COMPLEX  
 $[\text{Pt}(\text{en})_2][\text{Pt}(\text{en})_2\text{Cl}_2](\text{ClO}_4)_4$ ,  $\text{en}=\text{NH}_2\text{CH}_2\text{CH}_2\text{NH}_2$

NORITAKA KURODA, MASAMICHI SAKAI, MASASHI SUEZAWA,  
YUICHIRO NISHINA, KOJI SUMINO AND MASAHIRO YAMASHITA\*  
Institute for Materials Research, Tohoku University,  
Sendai 980, Japan

\*College of General Education, Nagoya University,  
Nagoya 464-01, Japan

**Abstract** The EPR experiments have been carried out to determine the ligands configurations of the paramagnetic valence anomalies created by UV irradiation in single crystals of  $[\text{Pt}(\text{en})_2][\text{Pt}(\text{en})_2\text{Cl}_2](\text{ClO}_4)_4$ ,  $\text{en}$  = ethylenediamine. The hyperfine and superhyperfine spectra show that the UV-induced valence anomalies are dimers of the nearest-neighbor Pt nuclei bearing either electron-like or hole-like spin. A variety of their dynamical properties are extracted from the temperature dependence of the quantum yield.

## INTRODUCTION

It is known that paramagnetic valence anomalies of  $S = 1/2$  are induced efficiently by the UV light irradiation of halogen-bridged linear chain complex  $[\text{Pt}(\text{en})_2][\text{Pt}(\text{en})_2\text{Cl}_2](\text{ClO}_4)_4$  ( $\text{en}$  = ethylenediamine) at low temperatures.<sup>1,2</sup> These valence anomalies consist of dimeric Pt ions,<sup>2,3</sup> and are highly mobile.<sup>2</sup> In the present work, their local structures and dynamical properties are studied in more details by the electron paramagnetic resonance (EPR) spectroscopy.

## EXPERIMENTAL PROCEDURES

The UV-induced EPR spectra are measured for single-crystalline samples by using a JEOL JES-FE2XG x-band spectrometer. The unpolarized radiation in the wavelength range 320–380 nm of a 300 W Xe-lamp is used as the light source of irradiation. The temperature of the sample is controlled with evaporated He gas. During the temperature-cycling experiments, the sensitivity of the spectrometer is calibrated by the EPR signal of a  $\text{MgO:Mn}^{2+}$  crystal which is placed in the ambient atmosphere at about 300 K inside the cavity.

## RESULTS AND DISCUSSION

### Local Structures of Paramagnetic Valence Anomalies

Figure 1 shows the spectrum obtained for  $H \parallel a$  at 20 K, where  $H$  denotes the magnetic field and  $a$  the  $a$ -axis of the crystal of the orthorhombic phase.

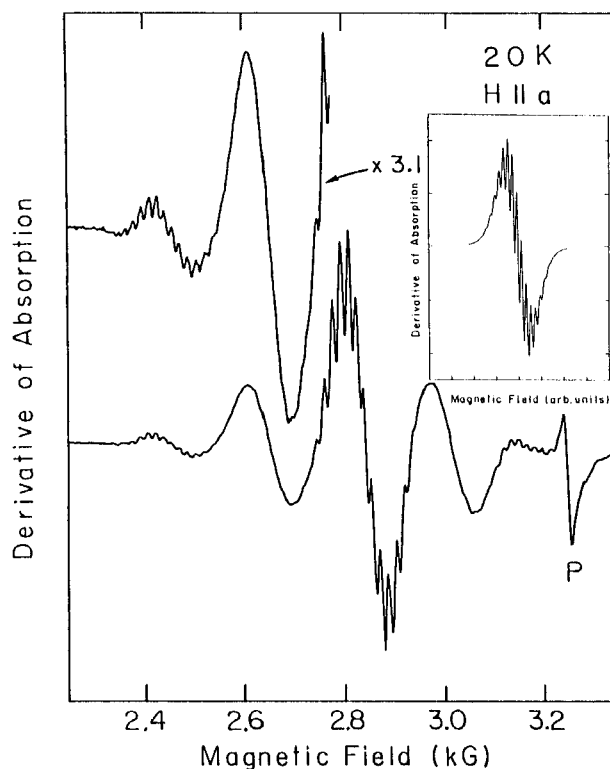


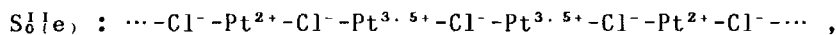
FIGURE 1 UV-induced EPR spectrum at 20 K for  $H \parallel a$ -axis. The line denoted as P is due to adhesive rayon paper used to fix the sample on a sample holder. The inset is a computer simulation of the superhyperfine pattern.

In this experiment, the sample is exposed first to the radiation at 80 K for about 100 min, and then cooled to 20 K while maintaining the sample in dark. The five symmetric resonance lines appearing in the field range 2.3–3.2 kG are the hyperfine structures due to dimeric Pt ions.<sup>2, 3, 4</sup> The main line around 2.8 kG is associated with the  $|0,0\rangle$

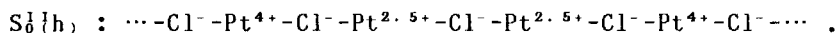
state in the representation  $|I, m\rangle$ , where  $I$  is the total nuclear angular momentum of the dimerized Pt nuclei and  $m$  is its magnetic quantum number. The next lines on the lower and higher field sides of the main line arise from the states  $|1/2, \pm 1/2\rangle$ , and the outermost two lines from  $|1, \pm 1\rangle$ . The  $|1, 0\rangle$  line is so weak that it is masked by the main line.

Each line is split into a doublet if the magnetic field is tilted from the  $ac$  plane. It is found from the angular dependence of the whole spectrum that there exist two kinds of unpaired spins; their principal axes,  $X$ ,  $Y$  and  $Z$ , are nearly parallel to the  $a$ ,  $c$  and  $b$  axes, respectively. In particular, within experimental error of  $\pm 0.5^\circ$ , the  $Z$  axis is parallel to the  $b$  axis which is the direction of the linear chain bonds.

For  $H \perp b$ , the  $|0, 0\rangle$  and  $|1, \pm 1\rangle$  lines exhibit clearly a superhyperfine splitting due to the interaction with ligands, as seen in Figure 1. To interpret the splitting, we employ the neutral soliton model proposed previously by the present authors,<sup>2</sup> since this model is consistent with the symmetry of the spin states clarified by the present work. In this model, the UV-induced paramagnetic valence anomalies are represented by the following structures:



and



UV radiation produces equal amounts of  $S_0^I\{e\}$  and  $S_0^I\{h\}$ . Taking account of the fact that four  $N^{3-}$  ions of ethylenediamine molecules ligate tightly to each Pt ion,<sup>5</sup> the ligands configurations of  $S_0^I\{e\}$  and  $S_0^I\{h\}$  can be designated as  $[(PtN_4Cl)_2]$  and  $[(PtN_4)_2]$ , respectively. The  $Cl^-$  ion at the center of each form is omitted on account of its rather loose bonding to Pt ions on either side as well as of its site symmetry. It is apparent from the observed spectrum that the superhyperfine constants,  $A^N$ s, of all the relevant  $^{14}N$  nuclei differ very little from each other and the ratio  $A^N/A^{Cl}$  is close to an integer or a reciprocal integer, where  $A^{Cl}$  is the superhyperfine constant of  $^{35,37}Cl$  nuclei of  $S_0^I\{e\}$ . The inset of Figure 1 shows the  $|0, 0\rangle$  spectrum obtained by a computer simulation for the case  $A^N/A^{Cl} = 1$  with a damping constant of  $0.8A^{N, Cl}$ . The

simulated spectrum reproduces the observed spectrum well as a whole, giving a strong support to the present interpretation. For  $H \parallel b$ , on the other hand, the  $Cl^-$  ion at the center of each form might not be negligible since the superhyperfine structure is smeared out regarding any hyperfine line even at a very low temperature.

#### Dynamical Properties

The  $|1/2, \pm 1/2\rangle$  lines in Figure 1 do not exhibit the superhyperfine splitting in contrast to the  $|0, 0\rangle$  and  $|1, \pm 1\rangle$  lines. It may be worth noting that, among many isotopes of Pt, only  $^{195}Pt$  has a nonvanishing nuclear angular momentum of  $1/2$ . The  $|1/2, \pm 1/2\rangle$  lines arise from dimers in which only one of constituent Pt nuclei is  $^{195}Pt$ . Hence, the absence of the superhyperfine structure of these lines implies that the spin density at the site of  $^{195}Pt$  is temporarily or spatially uncertain. In connection with a mobile character of these UV-induced spins,<sup>2</sup> the present observation suggests that the spins are fluctuating back and forth around their equilibrium positions except while they hop to the next positions.

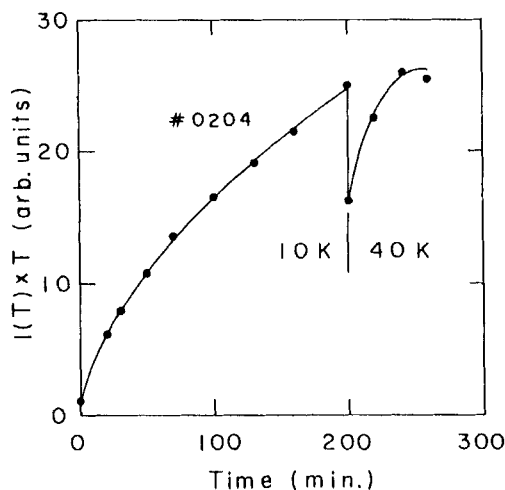


FIGURE 2 Evolution of the number of unpaired spins with exposure time at 10 K and 40 K. The number of spins is measured by the product  $I(T) \times T$ , where  $I(T)$  is the EPR intensity at temperature  $T$ .

According to the recent experiments on the quantum yield of the optically induced midgap absorption,<sup>6</sup> the midgap states can be created efficiently not only by the radiation polarized  $E \parallel b$ , but also by the radiation polarized  $E \perp b$ . Since the absorption coefficient is about  $100 \text{ cm}^{-1}$  for  $E \perp b$ , the midgap states are to be created in the surface region to a depth of about 0.1 mm. Figure 2 shows an experimental result of the quantum yield of unpaired spins, which is obtained by irradiating the ab surface of a crystal with a thickness of about 0.5 mm. A certain amount of spins are observed before irradiation because a pristine crystal of this material usually contains one unpaired spin per  $3 \times 10^3$  Pt atoms.<sup>3</sup> Note that a long exposure to radiation results in yielding more than 20 times as many spins as contained originally in the sample. It is of our particular interest that the yield rate is enhanced appreciably upon heating the sample from 10 K to 40 K. This result is comprehensible provided the spins can diffuse thermally towards inside of the crystal across the linear-chain bonds.

Figure 2 demonstrates another striking phenomenon. Namely, the

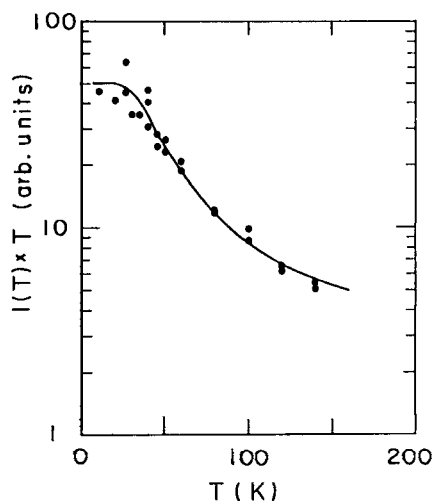


FIGURE 3 Temperature dependence of the number of unpaired spins. Solid circles are experimental values and the solid line is a theoretical curve.

spin number decreases if temperature is elevated from 10 K to 40 K in dark. Figure 3 shows the temperature dependence of the spin number measured in dark after the exposure at 40 K. As expected, the spin number decreases further with increasing temperature up to 140 K. It should be emphasized that, if temperature is lowered again to 40 K, the spin number recovers its initial level within the experimental error. There is no doubt that, at any temperature examined in the present work, the unpaired spins equilibrate thermally with a nonmagnetic state which lies a little higher in energy than the paramagnetic state in attention. Let this energy difference be  $\epsilon$ , the density of states of the nonmagnetic state relative to the paramagnetic state be  $\xi$ , and the spin number at 0 K be  $N_0$ . Then, the spin number at temperature  $T$  is given by

$$N(T) = N_0 / (1 + \xi e^{-\epsilon/kT}) , \quad (1)$$

where  $k$  is the Boltzmann constant. As shown in Figure 3, Equation (1) explains the experimental result satisfactorily if the values of  $\epsilon$  and  $\xi$  are chosen to be 14 meV and 25, respectively. The charged soliton state<sup>7</sup> is a candidate for the nonmagnetic state because the charged soliton is expected to be spin singlet and energetically very close to neutral soliton in the present material.<sup>8,9</sup>

## REFERENCES

1. S. Kurita and M. Haruki, Synth. Met., **29**, F129 (1989).
2. N. Kuroda, M. Sakai, M. Suezawa, Y. Nishina and K. Sumino, J. Phys. Soc. Jpn., **59**, 3049 (1990).
3. A. Kawamori, R. Aoki and M. Yamashita, J. Phys. C: Solid State Phys., **18**, 5487 (1985).
4. T. Krigas and M. T. Rogers, J. Chem. Phys., **55**, 3035 (1971).
5. N. Matsumoto, M. Yamashita, I. Ueda and S. Kida, Mem. Fac. Sci. Kyushu Univ., **C11**, 209 (1978).
6. K. Sato, M. Sakai, N. Kuroda, Y. Nishina and M. Yamashita, unpublished.
7. D. Baeriswyl and A. R. Bishop, J. Phys. C: Solid State Phys., **21**, 339 (1988).
8. A. Mishima and K. Nasu, Phys. Rev., **B39**, 5758 (1989).
9. N. Kuroda, M. Kataoka and Y. Nishina, Phys. Rev., **B**, in press.